

Received September 01, 2020; reviewed; accepted October 22, 2020

Halloysite intercalated by potassium acetate

Mariusz Adamczyk, Katarzyna Małycha, Karol Kułacz, Michał Pocheć, Kazimierz Orzechowski

Faculty of Chemistry, University of Wrocław, Joliot-Curie 14. 50-383 Wrocław, Poland

Corresponding author: kazimierz.orzechowski@chem.uni.wroc.pl (Kazimierz Orzechowski)

Abstract: Halloysite was intercalated by the mechanochemical technique from dry components. The process efficiency of 50% was achieved. The obtained intercalate differed from the material acquired using an aqueous solution of potassium acetate. The material was analyzed employing electron microscopy, thermogravimetry, X-ray powder diffraction, and dielectric spectroscopy. It was found that the molecules and/or ions present in the interlayer spaces retain some possibility of movement. This property of the material is promising for potential application as low expensive absorbers of electromagnetic radiation.

Keywords: clay minerals, electron microscopy, XRD, TGA, dielectric spectroscopy

1. Introduction

An interesting property of clay minerals is their ability to interact with inorganic and organic substances (Cheng et al., 2011; Frost, 1997; R. L. Frost et al., 2000b; Song et al., 2014). This can occur through adsorption on the surface of the mineral grains, cation exchange or intercalation (Frost et al., 1999; Joussein et al., 2005). The intercalation of halloysite involves the penetration of guest molecules between the mineral packets, which breaks the hydrogen bonds between tetrahedral and octahedral layers and creates new bonds between the host (mineral) and the guest. They are not stoichiometric chemical compounds and can be classified as bertolids. This process increases the distance between packets and could be observed on powder diffractograms. Physicochemical properties of the resulting intercalates are different than those of the original materials. Intercalates are interesting for pure science and have many industrial applications, for example in thermal storage (Song et al., 2014), in medicine (Joshi et al., 2009; Lin et al., 2002), as nanofillers and fireproof materials (Costa et al., 2007; Pereira et al., 2009), in catalysis (Chen et al., 2004; Garrido-Ramírez et al., 2010), in protection against electromagnetic radiation (Adamczyk et al., 2014; Kułacz and Orzechowski, 2019).

Comprehensive studies of intercalates with potassium acetate were carried out for halloysite (Cheng et al., 2011; Frost, 1997; R. L. Frost et al., 2000b) and kaolinite (Cheng et al., 2012; Franco and Cruz, 2004; Frost et al., 2001, 1998; Ray L. Frost et al., 2000). Taking into account the high similarity between kaolinite and halloysite it can be expected that the main conclusions are valid for both of them. The main difference between kaolinite and halloysite is the morphology and water content (Tari et al., 1999). Halloysite is usually coiled into tubes, contains additional interlayer water and can be easily modified during intercalation. It was found that acetate ions form different types of connections. At lower temperatures (below 50°C), the acetate ion can bind to the aluminum-oxygen-hydrogen layer through an additional water molecule, so that the intercalation distance can be as high as 14 Å. At higher temperatures, water is removed and the acetate ion binds directly to the aluminum-oxygen-hydroxide layer, taking a position perpendicular to the layer, resulting in an inter-packet distance of about 11.5 Å. The acetate ion can also take a position parallel to the layer, which results in an interplanar distance of about 9 Å. Potassium ions are located in the ditrigonal cavity of the gibbsite

layer. Electrostatic interactions between the potassium and acetate ions stabilize the intercalate and facilitate its formation.

In this paper, we present the results of physicochemical tests of halloysite intercalated by potassium acetate. We performed a qualitative and quantitative analysis using electron microscopy, thermogravimetric measurements and X-ray powder diffraction (XRD). The main part of the work was devoted to dielectric measurements. These studies were aimed at establishing the dynamics of guest particles trapped between the layers of mineral. This issue could be important in the context of possible applications of intercalated clay minerals as cheap and effective absorbers of electromagnetic radiation (Adamczyk et al., 2014; Kułacz and Orzechowski, 2019).

2. Materials and methods

Halloysite used for preparing the intercalate was obtained from the "Dunino" mine near Legnica, Poland. It is a tubular mineral of volcanic origin of a dark brown color. The specific surface area, SBET, is 60.9 m²/g, average diameter of pores, 122.3 Å, pores capacity, 0.19 cm³/g, and cationic capacity, CEC, 55 (Legocka et al., 2013). Halloysite was washed by demineralized water, centrifuged, and dried in air. The halloysite-potassium acetate intercalate was obtained by the mechanochemical method. Solid, dry halloysite and solid potassium acetate were mixed in 1:1 weight proportion and milled in the ball mill for several hours. The obtained material was washed many times with ethanol and dried in air at room temperature. The dry intercalate was rubbed and sealed tightly.

Electron microscopy was performed using a Hitachi S - 3400N Scanning Electron Microscope with an EDS Thermo Scientific Ultra Dry detector. The equipment made it possible to perform a quantitative and qualitative analysis in the selected area.

XRD measurements were performed using a powder diffractometer, D8 ADVANCE, with a copper lamp (Cu K α , wavelength $\lambda = 1.5418$ Å) and a Vantec detector. Measurements were carried out at room temperature in the range of angles 2θ 5-30° with a step of 0.05°.

Thermogravimetric analysis (TGA) and differential thermal analysis (DTA) were performed on a Setaram's SETSYS 16/18 instrument within the temperature range of 20-800°C, with a 5°C/min increment, in inert gas (N₂) atmosphere. The accuracy of mass change measurement was ± 0.005 mg and the temperature measurement accuracy was ± 0.2 °C.

Dielectric measurements were performed within the frequency range from 100 Hz to 1 MHz using a HP Precision LCR Meter HP4284A. Before the measurements, the instrument was calibrated according to the manufacturer's recommendations. In order to make the measurements more accurate, an additional compensation for stray capacitance was made based on the measurements of a Teflon pellet. No correction for field heterogeneity at the edges of the capacitor was applied.

Samples for dielectric measurements have a form of pellets. The pellets were prepared in a hydraulic press under a pressure of 30 kN/cm². The copper electrodes were glued to the pellets using a conductive adhesive. The resolution of ϵ' and ϵ'' measurements (respectively real and negative imaginary components of the electric permittivity) was 3%, absolute error could reach 15%.

3. Results and discussion

The investigation of the structure of halloysite intercalate with potassium acetate and its quantitative and qualitative analysis were carried out using a scanning electron microscope. We found the following mass content: C- (4.96 \pm 0.11)%; O - (55.54 \pm 0.73)%; Al - (14.55 \pm 0.08)%; Si - (14.84 \pm 0.08)%; P - (0.28 \pm 0.03)%; K- (4.18 \pm 0.03)%; Ti - (0.52 \pm 0.02)%; Fe - (5.02 \pm 0.06)%. The surface analysis showed the presence of potassium, coming probably from the intercalated compound. This means that a part of the intercalant is absorbed on the grain surface, which is likely to affect the dielectric properties of the material, resulting in a significant increase in DC conductivity. The presented photo (Fig. 1) shows that intercalate grains have a diameter of few micrometers and are in the form of bent plates.

Fig. 2 presents a powder diffraction pattern of halloysite intercalate with potassium acetate. Two characteristic reflections can be seen: one at $2\theta = 7.46^\circ$, associated with the intercalate, and the other at $2\theta = 12.28^\circ$, associated with natural halloysite. The calculated value of d_{001} of intercalate is 11.84 Å and that of halloysite is 7.20 Å. XRD measurements of halloysite intercalate with potassium acetate were already performed by Frost and co-workers (R. L. Frost et al., 2000a). The authors observed that

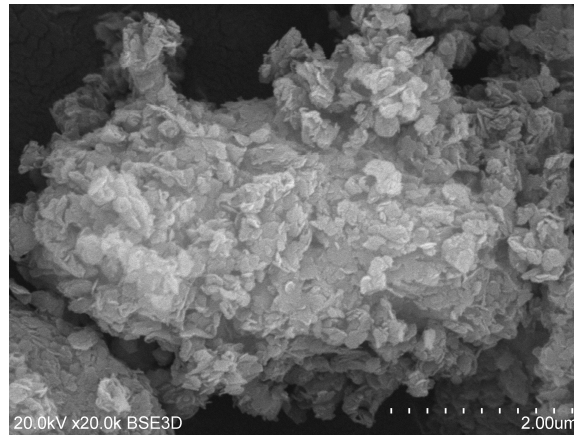


Fig. 1. The microscopic picture of halloysite intercalate with potassium acetate taken with a scanning electron microscope

after intercalation the lattice constant d_{001} increased to 13.97 Å. However, they also showed that the heating of the obtained intercalate to 250°C led to the occurrence of two forms, one characterized by $d_{001}= 11.72$ Å and the other, 8.89 Å. The lattice constant d_{001} obtained in our experiment is close to that of the larger d_{001} obtained by Frost et al. after heating. We suspect that the reason for the difference in lattice constant of the material obtained by Frost and co-workers and the material obtained in our investigations is another method of preparing the material. Frost et al. mixed the halloysite with an aqueous solution of potassium acetate, whereas we used the mechanochemical technique, which consists in grinding dry, solid components for a long time. The results show that the method used in these investigations leads directly to a form with a lattice constant of 11.9 Å. The intercalate obtained by Frost et al. is likely to contain additional water in the interlayer spaces, removed when heated to 250°C.

The efficiency of the mechanochemical method is not 100%, as evidenced by the presence of the reflex corresponding to the constant d_{001} equal to 7.2 Å (unmodified mineral). The comparison of the reflex intensity d_{001} for the intercalate (11.84 Å) and unmodified halloysite (7.20 Å) allows us to estimate the intercalation efficiency, according to the following formula (Stoch, 1974)

$$w_{XRD} = \frac{I(d_{001} \text{ int})}{I(d_{001} \text{ int}) + I(d_{001} \text{ hal})} \cdot 100\% \quad (1)$$

where $I(d_{001} \text{ int})$ is the reflex intensity of intercalate and $I(d_{001} \text{ hal})$, of halloysite. The efficiency of intercalation was estimated at 50%. The expansion of layers caused by intercalation was equal to 11.84 Å - 7.20 Å = 4.64 Å. This value correlates with the dimensions of the intercalated molecule. The long axis of acetate ions, estimated using HyperChem package, is 3.1 Å, whereas a distance between oxygen atoms, 2.1 Å. It suggests that the acetate ion can even take a position perpendicular to the layer. It is consistent with literature announcements (Frost, 1997). The large spacing of layers in relation to the particle dimensions proves the possibility of movement of the intercalant.

Fig. 3 shows thermogravimetric results for the studied intercalate. Three weight drops are visible. The first one starts practically at room temperature and extends to 146°C, and it is associated with the mass loss of 1.8%. This mass loss is accompanied by an endothermic peak centered at 71°C. We suspect that this process could be linked to the loss of water present in the pores of the mineral (Yuan et al., 2012) and, possibly, the removal of some ethanol used in the preparation of the material. The second mass loss (9.9%) is observed up to ca. 400°C and it is accompanied by an endothermic peak centered at 353°C. Based on the results of the study of the kaolinite intercalate with potassium acetate (Hofmann et al., 1934) it can be concluded that the release of water bound to potassium acetate as well as the de-intercalation and partial escape of potassium acetate are responsible for this weight loss. The third mass loss occurs between 400°C and 520°C (5.8%). The DTA curve shows two overlapping endothermal peaks. The occurrence of two effects is presumed: dehydroxylation of halloysite and decarboxylation of potassium acetate to carbonate (Ray L. Frost et al., 2000). Although potassium acetate have left the inter-packet space, they could be absorbed on the surface of the grains. The total weight loss of halloysite-potassium acetate intercalates from room temperature to 800°C is 18.9%.

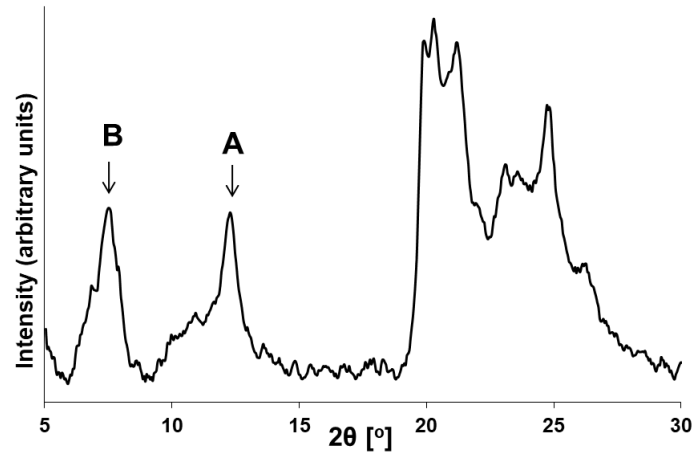


Fig. 2. Diffractogram of powder of halloysite intercalated with potassium acetate. A- d001 reflection of natural halloysite, B - d001 reflection of halloysite intercalated by potassium acetate. Over 18° overlapping reflections of d110 and d002 and possibly some reflections from gibbsite and quartz are visible. The spectrum presented on the figure was obtained after subtraction of the background from the original spectrum

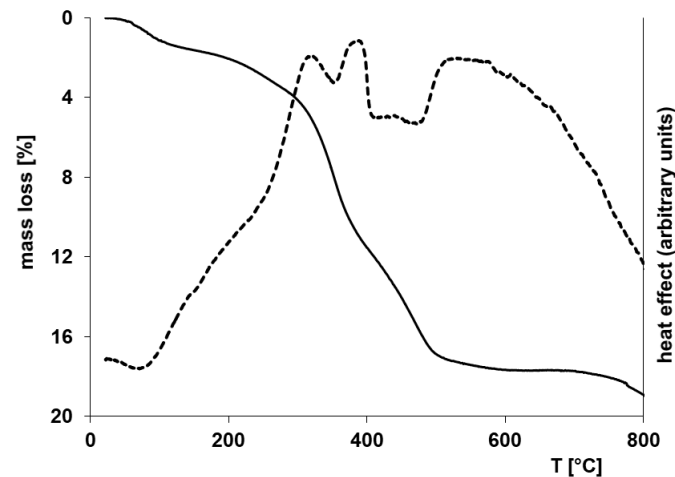


Fig. 3. TGA and DTA curves for the intercalate of halloysite with potassium acetate. Solid line - mass loss, dotted line - thermal effect

Studies of the surface of intercalate (electron microscopy), its internal structure (XRD), and thermal transformations (TG) provide valuable information on the material structure. However, to learn about the dynamics and movement of molecules, especially those placed in the mineral layers, we have applied dielectric spectroscopy. Measurements of dielectric properties of pellet samples lead to apparent quantities, depending on the packing of the samples. To make the results independent of the packing, the Robinson formula was used (Robinson, 2004):

$$\varepsilon' = \frac{\varepsilon'_{app} - \varepsilon_{air}(1-\varphi)}{\varphi}, \quad \varepsilon'' = \frac{\varepsilon''_{app}}{\varphi} \quad (2)$$

where ε_{air} is the relative permittivity of air ($\varepsilon_{air} = 1$), ε' - the real part of electric permittivity, ε'' - the negative imaginary part of electric permittivity, ε'_{app} - apparent value of real part of electric permittivity (obtained directly from the experiments), ε''_{app} - apparent value of negative imaginary part of electric permittivity (obtained directly from the experiments), $\varphi = d_x/d_i$ is the degree of filling of the capacitor with a sample, calculated as the ratio between the density of sample d_x (obtained from the mass and geometry of the pellet) and d_i , the estimated density of the crystalline intercalate. The density of crystalline intercalate was estimated from XRD and TG measurements as follows:

$$d_i = d_h \cdot (1 - w_{XRD}) + d_h \left(\frac{w_{XRD}}{w_{XRD} - w_{TG}} \right) \cdot \frac{d_{001}(hal)}{d_{001}(int)} \cdot w_{XRD} \quad (3)$$

where d_h is the density of halloysite (2.57 g/cm^3 (Mitra and Bhattacharjee, 1975)), $d001(hal)$, $d001(int)$ – $d001$ constants of halloysite and intercalate, respectively, w_{TG} – the ratio of the mass of the guest to the mass of the whole sample (determined from the TG curve), w_{XRD} – the efficiency of the intercalation calculated from XRD using equation 1.

Figs. 4-7 show the dielectric dispersion and absorption curves. The first two illustrate the low temperature range ($-100^\circ\text{C} \div 50^\circ\text{C}$) and the next two, the high temperature range ($50^\circ\text{C} \div 110^\circ\text{C}$). In our opinion, two relaxation processes are observed, the first one visible in the low temperature range and the other in the high temperature range. For the low temperature process, we can see that the maximum of absorption curves moves towards higher frequencies as the temperature increases, and for temperatures higher than 50°C it leaves the tested frequency window. For the high temperature process the relaxation time is much longer and the absorption maxima move generally towards the higher frequencies as the temperature increases, but this trend is not precisely fulfilled at all temperatures. The temperature dependence of permittivity is shown in Figs. 8 and 9. The ϵ' increases with an increase in temperature, but after the temperature of 40°C - 50°C is exceeded, it starts to drop. The ϵ'' also presents the maximum, and the position of the maximum is strongly dependent on frequency.

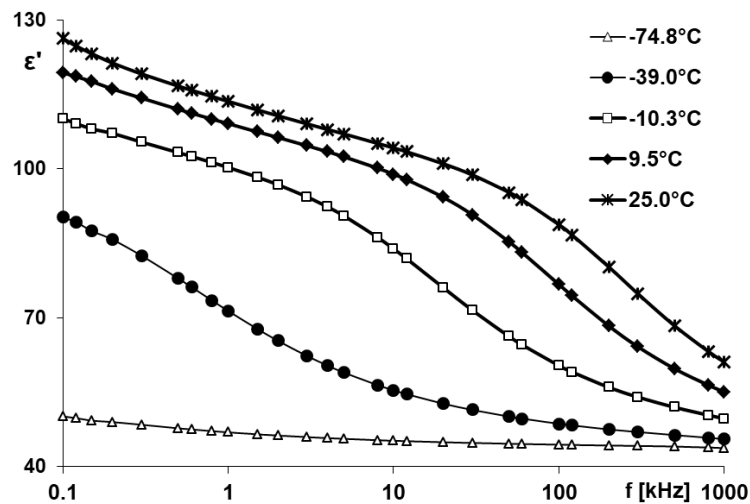


Fig. 4. Real component of electric permittivity as a function of frequency for selected temperatures – low temperature region

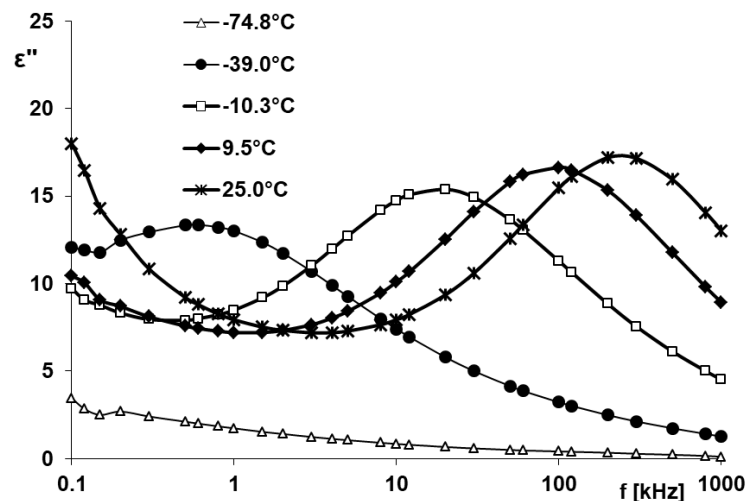


Fig. 5. Imaginary component of electric permittivity as a function of frequency for selected temperatures – low temperature region

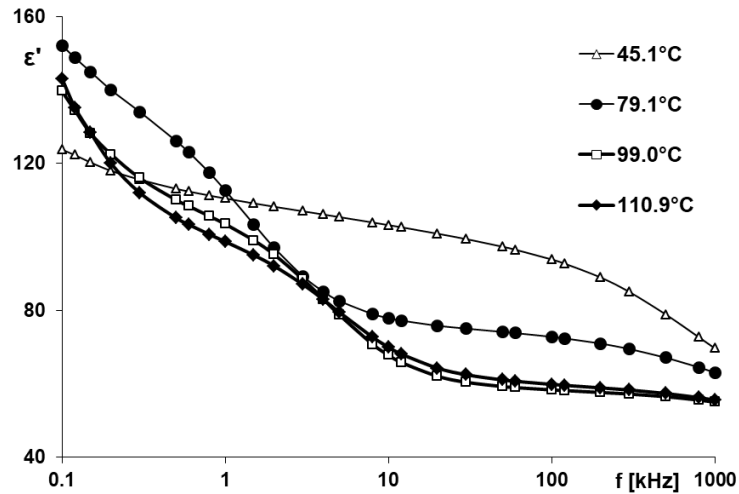


Fig. 6. Real component of electric permittivity as a function of frequency for selected temperatures - high temperature region

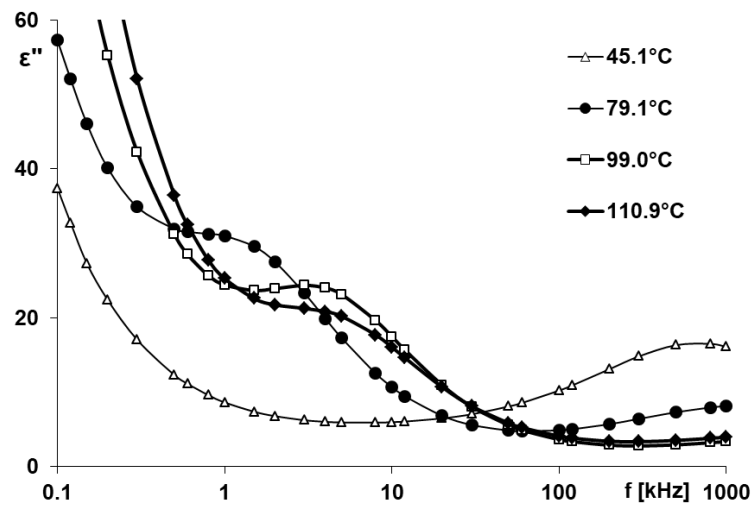


Fig. 7. Imaginary component of electric permittivity as a function of frequency for selected temperatures - high temperature region

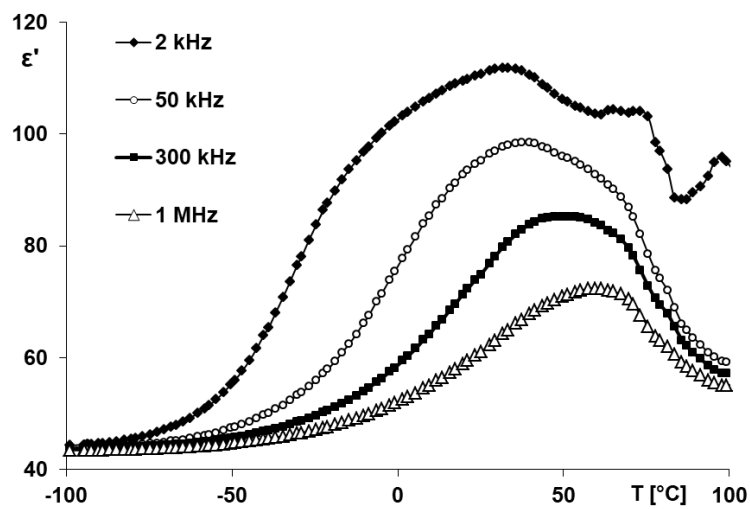


Fig. 8. Real component of electric permittivity as a function of temperature for selected frequencies

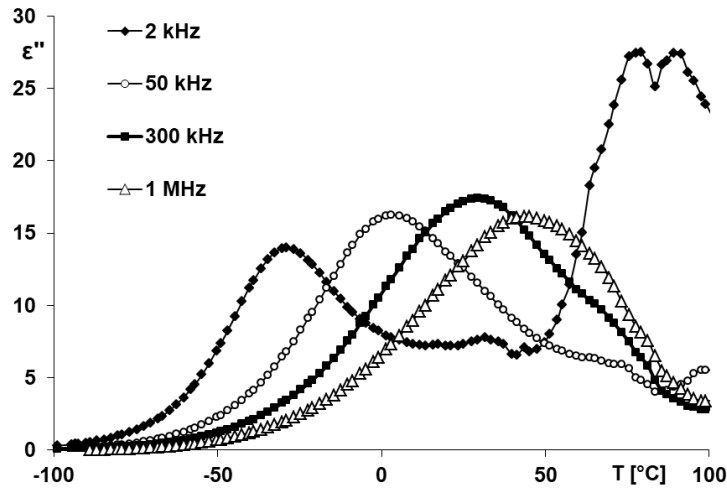


Fig. 9. Negative imaginary component of electric permittivity as a function of temperature for selected frequencies

In order to analyze the observed relaxations it will be useful to assume relaxation model and to fit the theoretical equation to the experimental points. From the previous papers, devoted to the halloysite-formamide intercalate (Adamczyk et al., 2014) and nontronite-formamide intercalate (Kułacz and Orzechowski, 2019), we learnt that the relaxation had a complicated form consisting of relaxation processes with distributed relaxation time (Havriliak-Negami equation), supplemented by conductivity and polarization terms. The fitting of such equation requires matching a large number of parameters which results in a large correlation among them and, consequently, in a high uncertainty of the fitted parameters. We have decided to apply a simplified method of estimating the macroscopic relaxation time, which consists in determining the frequency for which the maximum of the dielectric loss curve ($\epsilon''(f)$) occurs. This method of estimation of the relaxation time relies on the assumption about the mono-dispersive character of the relaxation process or a process with symmetrically distributed relaxation time. We hope that the method used to estimate the relaxation time would allow us to obtain qualitatively correct conclusions. Fig. 10 shows the relationship between the $\ln(T\tau)$ (logarithm of the product of temperature and macroscopic relaxation time) and $1000/T$ for the relaxation process observed at low temperatures. We can see that the Eyring equation was not met over the entire temperature range. It is possible to match the obtained data with two lines characterized by different activation energies: 71.7 kJ/mol in the temperature interval from -43°C to -25°C , and 36.7 kJ/mol in the temperature interval from -25°C to 45°C .

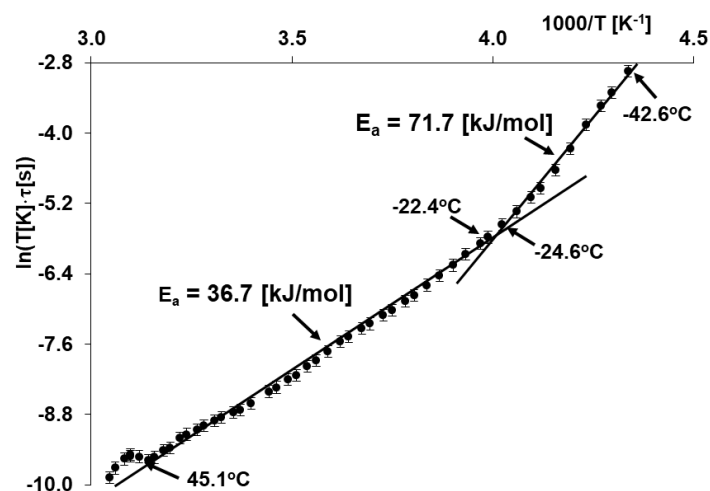
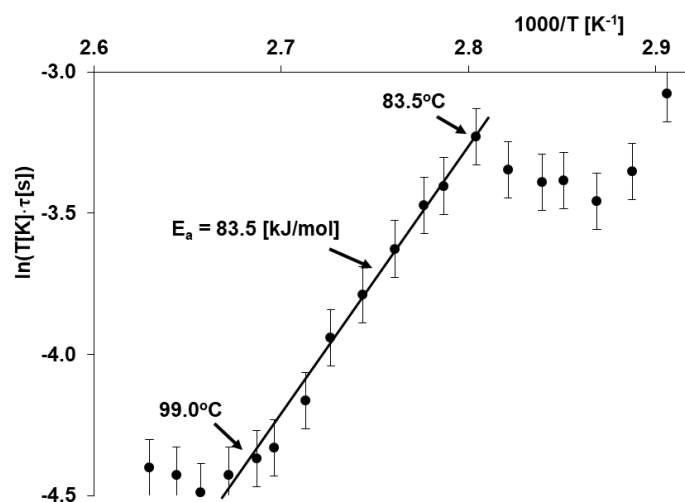


Fig. 10. $\ln(T\tau)$ as a function of $1000/T$ for halloysite intercalate with potassium acetate in the temperature range -42.6°C – 45.1°C

In our opinion, the relaxation characterized by 71.7 kJ/mol activation energy could be linked to the intercalated potassium acetate. It was concluded from Raman studies that acetate anions were bound both to the siloxane tetrahedral layer and gibbsite-like layers (Frost, 1997). The relatively large activation energy of dielectric relaxation confirms the qualitatively firm fixing of acetate ions between the layers. The relaxation dominant in the dielectric spectrum in the temperature range $-22.6^{\circ}\text{C} \div 45.1^{\circ}\text{C}$ and characterized by an activation energy of 36.7 kJ/mol can be associated with water present in the halloysite layers. A similar process was also found in natural halloysite (Adamczyk, 2014).

In Fig. 11 we analyzed the relaxation time for the process observed in the high temperature range $71\text{--}107^{\circ}\text{C}$. The Eyring equation is fulfilled within a limited temperature range only, from 83.5°C to 99.0°C . The activation energy is 83.5 kJ/mol. We linked this relaxation once again to the presence of potassium acetate, as observed at the temperature range from -43°C to -25°C , and then hidden by the relaxation of water. The estimated activation energy is even higher than before (71.7 kJ/mol). The removal of water probably makes the movement of acetate molecules more difficult.



- CHEN, B., LIU, J., CHEN, H., WU, J., 2004. *Synthesis of Disordered and Highly Exfoliated Epoxy/Clay Nanocomposites Using Organoclay with Catalytic Function via Acetone-Clay Slurry Method*. Chemistry of Materials 16, 4864-4866.
- CHENG, H., LIU, Q., YANG, J., MA, S., FROST, R.L., 2012. *The thermal behavior of kaolinite intercalation complexes - A review*. Thermochimica Acta 545, 1-13.
- CHENG, H., LIU, Q., YANG, J., ZHANG, J., FROST, R.L., DU, X., 2011. *Infrared spectroscopic study of halloysite-potassium acetate intercalation complex*. Journal of Molecular Structure 990, 21-25.
- COSTA, F.R., WAGENKNECHT, U., HEINRICH, G., 2007. *LDPE/Mg-Al layered double hydroxide nanocomposite: Thermal and flammability properties*. Polymer Degradation and Stability 92, 1813-1823.
- FRANCO, F., CRUZ, M.D.R., 2004. *Factors influencing the intercalation degree ('reactivity') of kaolin minerals with potassium acetate, formamide, dimethylsulphoxide and hydrazine*. Clay Min. 39, 193-205.
- FROST, R.L., 1997. *Intercalation of Halloysite: A Raman Spectroscopic Study*. Clays and Clay Minerals 45, 551-563.
- FROST, R. L., KRISTOF, J., HORVATH, E., KLOPROGGE, J.T., 2000a. *Rehydration and Phase Changes of Potassium Acetate-Intercalated Halloysite at 298 K*. Journal of Colloid and Interface Science 226, 318-327.
- FROST, R.L., KRISTOF, J., HORVATH, E., KLOPROGGE, J.T., 1999. *Deintercalation of dimethylsulphoxide intercalated kaolinites - a DTA/TGA and Raman spectroscopic study*. Thermochimica Acta 327, 155-166.
- FROST, R. L., KRISTOF, J., MAKO, E., KLOPROGGE, J.T., 2000b. *Modification of the hydroxyl surface of potassium acetate intercalated halloysite between 25 and 300 degrees C*. Am. Miner. 85, 1735-1743.
- FROST, R. L., KRISTOF, J., MAKO, E., KLOPROGGE, J.T., 2000. *Modification of the Hydroxyl Surface in Potassium-Acetate-Intercalated Kaolinite between 25 and 300 °C*. Langmuir 16, 7421-7428.
- FROST, R.L., KRISTOF, J., PAROZ, G.N., TRAN, T.H., KLOPROGGE, J.T., 1998. *The role of water in the intercalation of kaolinite with potassium acetate*. Journal of Colloid and Interface Science 204, 227-236.
- FROST, R.L., LOCOS, O.B., KRISTOF, J., KLOPROGGE, J.T., 2001. *Infrared spectroscopic study of potassium and cesium acetate-intercalated kaolinites*. Vibrational Spectroscopy 26, 33-42.
- GARRIDO-RAMIREZ, E.G., THENG, B.K.G., KORA, M.L., 2010. *Clays and oxide minerals as catalysts and nanocatalysts in Fenton-like reactions - A review*. Applied Clay Science 47, 182-192.
- HOFMANN, U., ENDELL, K., WILM, D., 1934. *Radiographic and colloid-chemical investigations of clay*. Angewandte Chemie 47, 0539-0547.
- JOSHI, G.V., KEVADIYA, B.D., PATEL, H.A., BAJAJ, H.C., JASRA, R.V., 2009. *Montmorillonite as a drug delivery system: Intercalation and in vitro release of timolol maleate*. International Journal of Pharmaceutics 374, 53-57.
- JOUSSEIN, E., PETIT, S., CHURCHMAN, J., THENG, B., RIGHI, D., DELVAUX, B., 2005. *Halloysite clay minerals - a review*. Clay Minerals 40, 383-426.
- KIŁACZ, K., ORZECZOWSKI, K., 2019. *Nontronite and intercalated nontronite as effective and cheap absorbers of electromagnetic radiation*. Dalton Trans. 48, 3874-3882.
- LEGOCKA, I., WIERZBICKA, E., AL-ZAHARI, T.M.J., OSAWARU, O., 2013. *Influence of halloysite on the structure, thermal and mechanical properties of polyamide 6*. Polimery 58, 24-32.
- LIN, F.H., LEE, Y.H., JIAN, C.H., WONG, J.M., SHEIH, M.J., WANG, C.Y., 2002. *A study of purified montmorillonite intercalated with 5-fluorouracil as drug carrier*. Biomaterials 23, 1981-1987.
- MITRA, G.B., BHATTACHERJEE, S., 1975. *The structure of halloysite*. Acta Crystallographica Section B Structural Crystallography and Crystal Chemistry 31, 2851-2857.
- PEREIRA, C.M.C., HERRERO, M., LABAJOS, F.M., MARQUES, A.T., RIVES, V., 2009. *Preparation and properties of new flame retardant unsaturated polyester nanocomposites based on layered double hydroxides*. Polymer Degradation and Stability 94, 939-946.
- ROBINSON, D.A., 2004. *Measurement of the solid dielectric permittivity of clay minerals and granular samples using a time domain reflectometry immersion method*. Vadose Zone Journal 3, 705-713.
- SONG, S., SONG, L., ZHANG, Y., CHEN, S., LI, Q., GUO, Y., DENG, S., SI, S., XIONG, C., 2014. *Lauric acid/intercalated kaolinite as form-stable phase change material for thermal energy storage*. Energy 76, 385-389.
- STOCH, L., 1974. *Mineralogija ilaste*. Wydawnictwa Geologiczne, Warszawa.
- TARI, G., BOBOS, I., GOMES, C.S.F., FERREIRA, J.M.F., 1999. *Modification of Surface Charge Properties during Kaolinite to Halloysite-7Å Transformation*. Journal of Colloid and Interface Science 210, 360-366.
- YUAN, P., TAN, D., AANNABI-BERGAYA, F., YAN, W., FAN, M., LIU, D., HE, H., 2012. *Changes in Structure, Morphology, Porosity, and Surface Activity Of Mesoporous Halloysite Nanotubes Under Heating*. Clays Clay Miner. 60, 561-573.